

Optimized Electron Transfer in Charge-Transfer Ion Pairs. Pronounced Inner-Sphere Behavior of Olefin Donors

Stephan M. Hubig, T. Michael Bockman, and Jay K. Kochi*

Contribution from the Department of Chemistry, University of Houston, Houston, Texas 77204-5641

Received December 18, 1995[⊗]

Abstract: Time-resolved (fs) spectroscopy allows the direct observation of charge-transfer ion pairs resulting from the photoexcitation of the electron donor–acceptor (EDA) complexes of tetracyanoethylene with various olefin donors, i.e., [olefin, TCNE], in dichloromethane solutions. Measurement of the spectral decays yields first-order rate constants for electron transfer (k_{ET}) in the collapse of the charge-transfer ion pairs [olefin⁺, TCNE⁻] by very rapid return to the ground-state EDA complex at 25 °C. [These ultrafast ET rates necessitated the design/construction of a new tunable, high-power pump–probe spectrometer based on a Ti:sapphire laser with 250-fs resolution.] The value of $k_{\text{ET}} = 5 \times 10^{11} \text{ s}^{-1}$ is strikingly nonvariant for the different TCNE complexes despite large differences in the driving force for electron transfer (ΔG_0), as evaluated from the varying ionization potentials of the olefins. Such a unique nonvariant trend for the free energy relationship ($\log k_{\text{ET}}$ versus ΔG_0) is analyzed in terms of a dominant inner-sphere component to electron transfer. In a more general context, the inner-sphere (adiabatic) electron transfer in [olefin⁺, TCNE⁻] relates to a similar, but less pronounced, inner-sphere behavior noted in the analogous [arene⁺, TCNE⁻] radical-ion pairs. As such, these electron-transfer processes represent an extremum in the continuum of ET transition states based on the inner-sphere/outer-sphere dichotomy.

Introduction

Recent developments in time-resolved spectroscopy allow the direct observation of very fast electron-transfer (ET) processes^{1,2} to probe the intermolecular interactions inherent to a full description of the transition state.³ In particular, the dynamic behavior of photogenerated radical-ion pairs has been studied extensively with a view to current electron-transfer theories.^{4–13} Perhaps the most intriguing result of these studies is that the

ET rates in radical-ion pairs generated by electron-transfer quenching of excited states show a distinct driving-force dependence as predicted by outer-sphere electron-transfer theories.^{4–8} In contrast, ET rates in radical-ion pairs generated by charge-transfer (CT) excitation of electron donor–acceptor (EDA) complexes (hereafter referred to as charge-transfer ion pairs) do not seem to follow the “bell-shaped” correlation.^{9–13} A second remarkable observation has been reported by several groups, namely, that ET rates in radical-ion pairs not only depend on the free-energy change of the redox process, but also on the type of the electron donors and acceptors, for example, n - or π -donors, and on the size of the π -system involved in the electron transfer.^{5,6,10} For instance, cation radicals derived from n -donors such as amines react faster when ion-paired with anion radicals than those derived from aromatic π -donors of comparable oxidation potentials.⁶ Furthermore, benzene cation radicals react faster than naphthalene or anthracene cation radicals of comparable oxidation potentials.^{5,10}

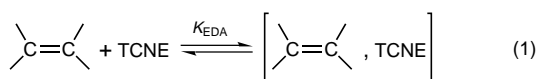
Various theoretical approaches have been suggested to account for these experimental results. Thus, the original outer-sphere electron-transfer model has been modified by allowing for (i) the variation in the solvation and Coulombic work terms,^{13–15} (ii) the variation in the reorganization energy terms,¹⁶ or (iii) the variation in the electronic coupling between donor and acceptor orbitals.¹⁷ Since all these parameters are highly dependent on the electron donor–acceptor distance, the most pronounced deviations are expected for radical-ion pairs consisting of relatively small π -donors and π -acceptors for which *ab initio* calculations predict a rather close intermolecular distance.¹⁸

- [⊗] Abstract published in *Advance ACS Abstracts*, April 1, 1996.
- (1) (a) Fleming, G. R. *Annu. Rev. Phys. Chem.* **1986**, *37*, 81. (b) Yoshihara, K.; Yartsev, A.; Nagasawa, Y.; Kandori, H.; Douhal, A.; Kemnitz, K. *Pure Appl. Chem.* **1993**, *65*, 1671. (c) Mataga, N. In *Electron Transfer in Inorganic, Organic, and Biological Systems*; Bolton, J. R., Mataga, N., McLendon, G., Eds.; American Chemical Society: Washington, DC, 1991; pp 91 f. (d) Closs, G. L.; Johnson, M. D.; Miller, J. R.; Piotrowiak, P. *J. Am. Chem. Soc.* **1989**, *111*, 3751. (e) Zaleski, J. M.; Turró, C.; Mussell, R.; Nocera, D. G. *Coord. Chem. Rev.* **1994**, *132*, 249. (f) Johnson, A. E.; Tominaga, K.; Walker, G. C.; Jarzaba, W.; Barbara, P. F. *Pure Appl. Chem.* **1993**, *65*, 1677.
- (2) (a) Kaiser, W. *Ultrashort Laser Pulses and Applications*; Springer: New York, 1988. (b) Martin, J.-L.; Migus, A.; Mourou, G. A.; Zewail, A. H. *Ultrafast Phenomena VIII*; Springer: New York, 1993.
- (3) (a) Grubele, M.; Zewail, A. H. *Phys. Today* **1990**, May, 24. (b) Zewail, A. H. *J. Phys. Chem.* **1993**, *97*, 12427.
- (4) (a) Mataga, N.; Asahi, T.; Kanda, Y.; Okada, T.; Kakitani, T. *Chem. Phys.* **1988**, *127*, 249. (b) Ohno, T.; Yoshimura, A.; Mataga, N. *J. Phys. Chem.* **1990**, *94*, 4871. (c) Gould, I. R.; Ege, D.; Mattes, S. L.; Farid, S. *J. Am. Chem. Soc.* **1987**, *109*, 3794.
- (5) Gould, I. R.; Ege, D.; Moser, J. E.; Farid, S. *J. Am. Chem. Soc.* **1990**, *112*, 4290.
- (6) Burget, D.; Jacques, P.; Vauthey, E.; Suppan, P.; Haselbach, E. *J. Chem. Soc., Faraday Trans.* **1994**, *90*, 2481.
- (7) (a) Vauthey, E.; Suppan, P.; Haselbach, E. *Helv. Chim. Acta* **1988**, *71*, 93. (b) Kikuchi, K.; Takahashi, Y.; Koike, K.; Wakamatsu, K.; Ikeda, H.; Miyashi, T. *Z. Phys. Chem. N. F.* **1990**, *167*, 27.
- (8) Levin, P. P.; Raghavan, P. K. N. *Chem. Phys. Lett.* **1991**, *182*, 663.
- (9) Asahi, T.; Mataga, N.; Takahashi, Y.; Miyashi, T. *Chem. Phys. Lett.* **1990**, *171*, 309.
- (10) Asahi, T.; Mataga, N. *J. Phys. Chem.* **1989**, *93*, 6575.
- (11) Asahi, T.; Mataga, N. *J. Phys. Chem.* **1991**, *95*, 1956.
- (12) Segawa, H.; Takehara, C.; Honda, K.; Shimidazu, T.; Asahi, T. *Mataga, N. J. Phys. Chem.* **1992**, *96*, 503.
- (13) Asahi, T.; Ohkohchi, M.; Mataga, N. *J. Phys. Chem.* **1993**, *97*, 13132.

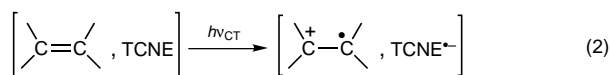
- (14) Tachiyu, M.; Murata, S. *J. Phys. Chem.* **1992**, *96*, 8441.
- (15) Kakitani, T.; Yoshimori, A.; Mataga, N. *J. Phys. Chem.* **1992**, *96*, 5386.
- (16) Gould, I. R.; Noukakis, D.; Gomez-Jahn, L.; Goodman, J. L.; Farid, S. *J. Am. Chem. Soc.* **1993**, *115*, 4405.
- (17) Tachiyu, M.; Murata, S. *J. Am. Chem. Soc.* **1994**, *116*, 2434.
- (18) Alvarez-Idaboy, J. R.; Eriksson, L. A.; Fångström, T.; Lunell, S. *J. Phys. Chem.* **1993**, *97*, 12737.

On the basis of these considerations, the classic electron acceptor tetracyanoethylene (TCNE) is the obvious choice. It is compact in size and has a very high acceptor strength, as defined by its well-known one-electron reduction potential in solution¹⁹ and its electron affinity in the gas phase.²⁰ It forms numerous EDA complexes with various types of electron donors, which have been characterized by UV-vis spectroscopy,^{21–24} Raman spectroscopy,^{25,26} and X-ray crystallography.^{24,27–30} The reduced anion radical TCNE^{•-} has been thoroughly examined in terms of its spectral features,³¹ structure,³² and spin-density distribution.³² On the other hand, kinetic studies on photoinduced electron transfer within the electron donor–acceptor complexes of TCNE are rather limited.^{10,11,33} As a result, the effect of the compact size of TCNE on the electron-transfer behavior in radical-ion pairs has not been explicitly addressed. The strongest effects of small π -systems on electron-transfer rates are expected when the TCNE acceptor is combined with the smallest π -donor, namely, an olefin.

In solution, various types of olefins readily form EDA complexes with tetracyanoethylene,^{21c,22} i.e.



Accordingly in this study, we will show that photoexcitation of these EDA complexes leads directly to the charge-transfer ion pair, i.e.



in analogy to the corresponding aromatic complexes.³³ These CT ion pairs are expected to collapse extremely fast by electron transfer from the TCNE anion radical to the olefin cation radical.

In order to monitor this ultrafast ion-pair collapse on the femtosecond and early picosecond time scale, we constructed

(19) Peover, M. E. *Trans. Faraday Soc.* **1966**, *62*, 3535.

(20) Drzaic, P. S.; Marks, J.; Braumann, J. I. In *Gas Phase Ion Chemistry*; Bowers, M. T., Ed.; Academic Press: Orlando, 1984; Vol. 3, p 167.

(21) (a) Frey, J. E.; Kitchen, E. C. *J. Am. Chem. Soc.* **1983**, *105*, 2175. (b) Frey, J. E.; Cole, R. D.; Kitchen, E. C.; Suprenant, L. M.; Sylwestrzak, M. S. *J. Am. Chem. Soc.* **1985**, *107*, 748. (c) Frey, J. E.; Andrews, A. M.; Ankoviac, D. G.; Beaman, D. N.; Du Pont, L. E.; Elsner, T. E.; Lang, S. R.; Oosterbaan, Z. M. A.; Seagle, R. E.; Torreano, L. A. *J. Org. Chem.* **1990**, *55*, 606. (d) Frey, J. E.; Andrews, A. M.; Combs, S. D.; Edens, S. P.; Puckett, J. J.; Seagle, R. E.; Torreano, L. A. *J. Org. Chem.* **1992**, *57*, 6460. (e) Frey, J. E.; Aiello, T.; Beaman, D. N.; Combs, S. D.; Fu, S.-L.; Puckett, J. J. *J. Org. Chem.* **1994**, *59*, 1817. (f) Frey, J. E.; Aiello, T.; Beaman, D. N.; Hutson, H.; Lang, S. R.; Puckett, J. J. *J. Org. Chem.* **1995**, *60*, 2891.

(22) Belysheva, G. V.; Egorochkin, A. N.; Sennikov, P. G.; Lopatin, M. A.; Voronenkov, V. V. *Bull. Acad. Sci. USSR, Div. Chem. Sci.* **1990**, *39*, 1181.

(23) Spange, S.; Maenz, K.; Stadermann, D. *Liebigs Ann. Chem.* **1992**, *1033*.

(24) Blackstock, S. C.; Poehling, K.; Greer, M. L. *J. Am. Chem. Soc.* **1995**, *117*, 6617.

(25) Britt, B. M.; McHale, J. L.; Friedrich, D. M. *J. Phys. Chem.* **1995**, *99*, 6347.

(26) Kulinowski, K.; Gould, I. R.; Myers, A. B. *J. Phys. Chem.* **1995**, *99*, 9017.

(27) Williams, R. M.; Wallwork, S. C. *Acta Crystallogr.* **1967**, *22*, 899.

(28) Larsen, F. K.; Little, R. G.; Coppens, P. *Acta Crystallogr.* **1975**, *B31*, 430 and references therein.

(29) Renault, A.; Cohen-Addad, C.; Lajzerowicz, J.; Canadell, E.; Eisenstein, O. *Mol. Cryst. Liq. Cryst.* **1988**, *164*, 179 and references therein. (30) Masnovi, J.; Baker, R. J.; Towns, R. L. R.; Chen, Z. *J. Org. Chem.* **1991**, *56*, 176.

(31) (a) Jeanmaire, D. L.; Suchanski, M. R.; Van Duyne, R. P.; *J. Am. Chem. Soc.* **1975**, *97*, 1699. (b) Webster, O. W.; Mahler, W.; Benson, R. E. *J. Am. Chem. Soc.* **1962**, *84*, 3768. (c) Itoh, M. *J. Am. Chem. Soc.* **1970**, *92*, 887. (d) Shida, T. *Electronic Spectra of Radical Ions*; Elsevier: Amsterdam, 1988.

Table 1. Electron Donor–Acceptor Complexes of Tetracyanoethylene with Various Olefins^a

olefin donor	IP (eV)	λ_{CT}^b (nm)	k_{ET}^c (s ⁻¹)
3,3-dimethyl-1-butene	9.67 ^d	340	4.6×10^{11}
1-hexene	9.48 ^e	360	2.9×10^{11}
2,3-dimethyl-1-butene	9.11 ^d	400	6.4×10^{11}
2-hexene	8.95 ^d	420	4.5×10^{11}
norbornene	8.95 ^f	420	5.0×10^{11}
2,4,4-trimethyl-2-pentene	8.83 ^d	438	4.2×10^{11}
2,5-dimethyl-2-hexene	8.65 ^d	466	4.9×10^{11}

^a In dichloromethane solution at 25 °C. ^b Spectral maximum of the CT absorption band of the 1:1 complex of TCNE with the olefin donor identified in column 1. ^c Rate constants for electron transfer following the CT excitation of the olefin/TCNE complex at 375 or 400 nm. ^d Interpolated value from the Mulliken correlation³⁴ in Figure 1A. ^e Reference 46a. ^f Reference 46b.

a new time-resolved pump–probe spectrometer (as described herein) based on a self-mode-locked Ti:sapphire oscillator. The laser system generated 250-fs high-energy pulses, continuously tunable between 720 and 920 nm, at low repetition rate. Complete, well-resolved transient spectra, over a wavelength range from 360 to 900 nm, could be recorded in a single shot.

Results

I. Formation of Olefin Complexes with Tetracyanoethylene. When a colorless solution (0.02 M) of tetracyanoethylene in dichloromethane and neat *trans*-2-hexene were mixed, a bright yellow color developed immediately. UV-vis spectroscopy revealed that the yellow color was caused by a new absorption band in a wavelength range where neither the olefin nor TCNE absorbed. The new absorption band with a maximum at 420 nm was ascribed to the charge-transfer transition^{21c} arising from the formation of the electron donor–acceptor (EDA) complex between *trans*-2-hexene and TCNE according to eq 1. Similar colorations, varying between slightly yellow and dark purple, were observed with other olefins. The maxima of the CT absorption bands, λ_{CT} in Table 1, ranged from 340 nm for 3,3-dimethyl-1-butene to 540 nm for 2,3-dimethyl-2-butene. The plot of the charge-transfer energies $E_{\text{CT}} = hc/\lambda_{\text{CT}}$ versus the ionization potential of the olefin, IP, in Figure 1A yielded a slope of nearly unity ($s = 0.97$), in excellent agreement with the Mulliken correlation³⁴ in eq 3, where IP and EA represent

$$E_{\text{CT}} = hc/\lambda_{\text{CT}} = \text{IP} + \text{EA} + \text{constant} \quad (3)$$

the ionization potential of the donor and the electron affinity of the acceptor, respectively. The analogous plot for the EDA complexes of various arenes with TCNE yielded a similar slope ($s = 0.90$; see Table 2 and Figure 1B).

II. Photoexcitation of the Electron Donor–Acceptor Complexes. a. TCNE and Olefin Donors. The charge-transfer absorption band of the EDA complexes of olefins with TCNE was irradiated at either 375 or 400 nm with a 250-fs laser pulse. The transient spectrum in Figure 2 with an absorption maximum at 450 nm was assigned to that of the tetracyanoethylene radical anion, in accord with that of authentic

(32) Zheludev, A.; Grand, A.; Ressouche, J.; Schweizer, J.; Morin, B. G.; Epstein, A. J.; Dixon, D. A.; Miller, J. S. *Angew. Chem., Int. Ed. Engl.* **1994**, *33*, 1397.

(33) (a) Hilinski, E. F.; Masnovi, J. M.; Amatore, C.; Kochi, J. K.; Rentzepis, P. M. *J. Am. Chem. Soc.* **1983**, *105*, 6167. (b) Hilinski, E. F.; Masnovi, J. M.; Kochi, J. K.; Rentzepis, P. M. *J. Am. Chem. Soc.* **1984**, *106*, 8071. (c) Wynne, K.; Galli, C.; Hochstrasser, R. M. *J. Chem. Phys.* **1994**, *100*, 4797.

(34) (a) Mulliken, R. S. *J. Am. Chem. Soc.* **1950**, *72*, 600. (b) Mulliken, R. S. *J. Am. Chem. Soc.* **1952**, *74*, 811. (c) Mulliken, R. S. *J. Phys. Chem.* **1952**, *56*, 801. (d) Mulliken, R. S.; Person, W. B. *Molecular Complexes*; Wiley: New York, 1969.

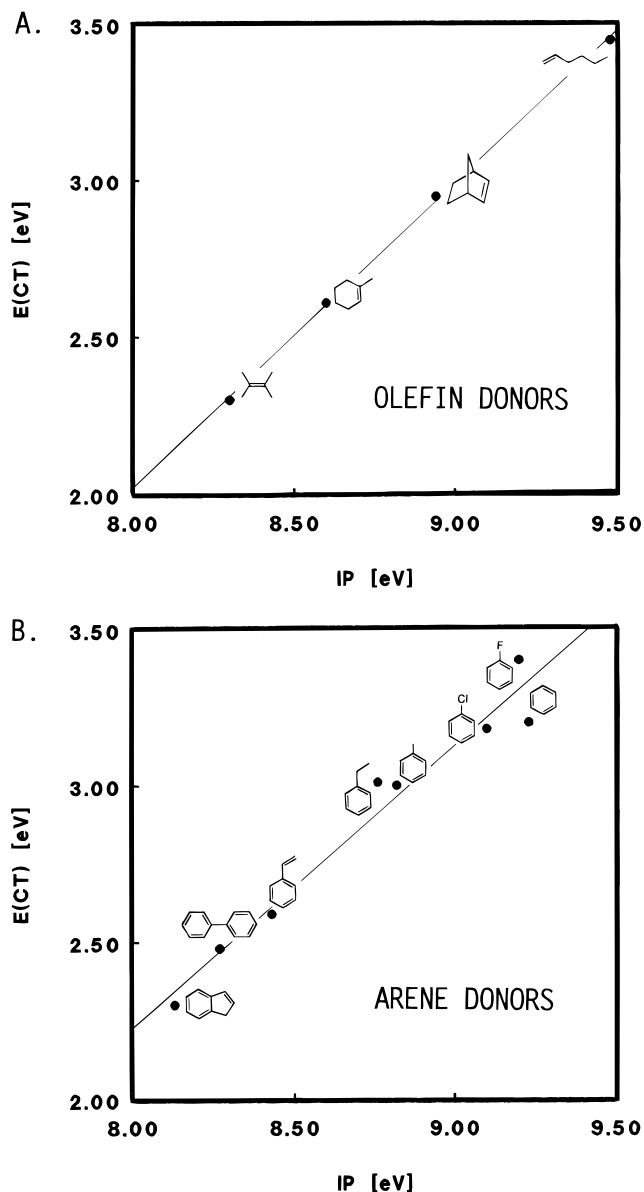


Figure 1. Mulliken correlation of the charge-transfer energies (E_{CT}) of various TCNE complexes in dichloromethane versus ionization potentials (IP) of (A) olefins and (B) arenes.

TCNE $^{\bullet-}$ reported previously.³¹ In all cases, the transient absorption band decayed completely to the baseline on the early picosecond time scale following first-order kinetics. The lifetime of $\tau = 2 \pm 0.4$ ps corresponded to a decay rate constant of $(4.6 \pm 0.9) \times 10^{11} \text{ s}^{-1}$ (see inset to Figure 2). A single (nonvariant) rate constant for first-order decay was sufficient to describe the kinetic behavior of all of the olefins in Table 1. It is singularly noteworthy that this rate constant did not depend on either the alkyl substitution or the donor strength of the olefin.

b. TCNE and Arene Donors. For comparison, the aromatic complexes with TCNE in dichloromethane were also excited with the 250-fs laser pulse at either 375 or 400 nm. The collapse of the charge-transfer ion pair was monitored by following the first-order decay of the TCNE $^{\bullet-}$ anion radical as described for the olefin complexes. In three cases (i.e., indene, styrene, and biphenyl), the transient absorption spectrum also showed a distinct absorption band of the arene cation radical (i.e., $\text{IN}^{\bullet+}$, $\text{STY}^{\bullet+}$, and $\text{BIP}^{\bullet+}$)^{31d} in addition to the TCNE $^{\bullet-}$ absorption band, as illustrated in Figure 3. The $\text{IN}^{\bullet+}$, $\text{STY}^{\bullet+}$, and $\text{BIP}^{\bullet+}$ absorption bands did not reveal any spectral distortions as compared to the spectra published elsewhere (see the Experi-

Table 2. EDA Complexes of Tetracyanoethylene with Various Arenes^a

arene donor	IP (eV)	λ_{CT}^b (nm)	k_{ET}^c (s $^{-1}$)
cyanobenzene	9.71 ^d	<i>e</i>	9.6×10^9
<i>m</i> -cyanotoluene	9.34 ^f	<i>e</i>	9.0×10^9
benzene	9.23 ^g	388	1.4×10^{10}
fluorobenzene	9.20 ^h	365	3.4×10^{10}
chlorobenzene	9.10 ^h	390	2.1×10^{10}
toluene	8.82 ^g	414	1.0×10^{11}
ethylbenzene	8.76 ^d	412	8.5×10^{10}
allylbenzene	8.76 ^f	412	1.2×10^{11}
styrene	8.43 ^d	397/480 ⁱ	2.0×10^{11}
biphenyl	8.27 ^k	400/500 ^j	1.9×10^{11}
indene	8.13 ^d	420/540 ^j	6.0×10^{11}

^a In dichloromethane at 25 °C. ^b Spectral maximum of the CT absorption band of the 1:1 complex of TCNE with the arene donor identified in column 1 (in dichloromethane). ^c Rate constants for electron transfer following CT excitation of the arene/TCNE complex at 375 or 400 nm. ^d Reference 47a. ^e Absorption tail observed. ^f Reference 47b. ^g Reference 48a. ^h Reference 50b. ⁱ Interpolated value from the Mulliken correlation³⁴ shown in Figure 1B. ^j Two CT absorption bands observed. ^k Reference 46b.

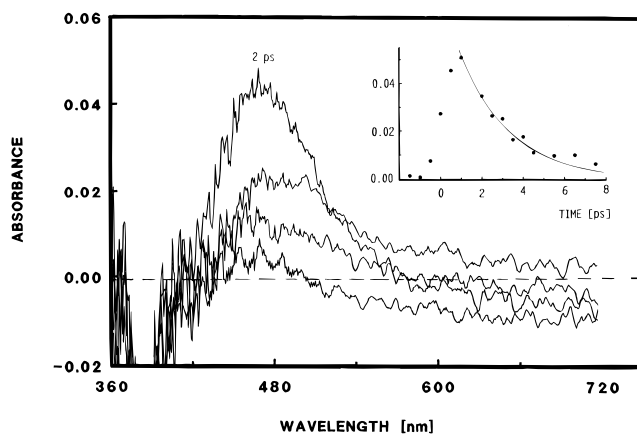


Figure 2. Transient absorption spectrum obtained at (from top to bottom) 2, 3, 4, and 5 ps following the 385-nm excitation of the TCNE complex of *trans*-2-hexene in dichloromethane with the 250-fs laser pulse. Inset: Spectral decay monitored at 470 nm. The smooth line shows the fit to first-order kinetics.

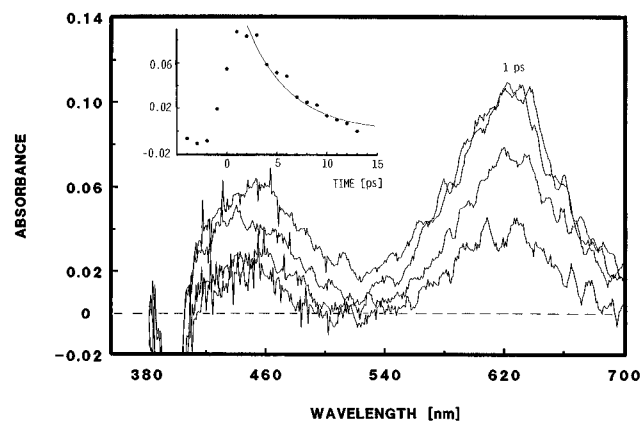
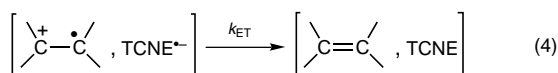


Figure 3. Transient absorption spectrum obtained at (from top to bottom) 1, 2, 4, and 6 ps following the 400-nm excitation of the TCNE complex of styrene in dichloromethane. Inset: Spectral decay monitored at 620 nm. The smooth line shows the fit to first-order kinetics.

mental Section). In all three cases, the transient spectra were analyzed as the sum of the absorption spectra of the radical cation and TCNE $^{\bullet-}$ and the negative absorbance (bleach) of the charge-transfer band of the ground-state EDA complex. The quantitative comparison of the absorption bands in the transient spectra established a 1:1 stoichiometry for the formation of the

arene cation radicals and the tetracyanoethylene anion radical. [See the Experimental Section for the details of this analysis.] The spectral observation of cation radical and anion radical allowed us to analyze the kinetics of the ion-pair collapse by using the first-order decay traces of both ion-pair partners. Both transients decayed to the spectral baseline at identical rates. On the basis of these results, we conclude that in all cases (e.g., olefin/TCNE and arene/TCNE complexes), the observed decay of the TCNE^{•-} absorption corresponded to electron transfer from the TCNE^{•-} anion radical to the donor cation radical, i.e.



and it resulted in the complete recovery of the ground-state EDA complex.³⁵

The first-order rate constants in Table 2 show that k_{ET} for arene/TCNE charge-transfer ion pairs varied nearly 2 orders of magnitude upon proceeding from cyanobenzene to indene. Thus, this trend was in strong contrast to the nonvariant electron-transfer behavior of olefins.

c. Olefins and Aromatic Acceptors. In order to obtain a general perspective of the ET kinetics of olefin complexes, we examined a series of analogous EDA complexes with three other electron acceptors, namely, pyromellitic dianhydride (PMDA), tetracyanobenzene (TCNB), and tetrachlorophthalic anhydride (TCPA). It should be noted that these aromatic acceptors differed from tetracyanoethylene in size as well as acceptor strength. Following the laser excitation at 400 nm, the spectral decay of the reduced acceptors was monitored at 665 nm for PMDA^{•-}, at 470 nm for TCNB^{•-}, and at 440 nm for TCPA^{•-}.^{31d} The electron-transfer rate constants in Table 3 varied over 1 order of magnitude depending on the driving force, ΔG_0 , for each donor-acceptor combination.

For a more general analysis of the driving-force dependence of electron-transfer rate constants in charge-transfer ion pairs (see the Discussion), several series of other complexes with benzenes, naphthalenes, and anthracenes as donors and tetracyanobenzene and methylviologen as acceptors were included in this study. The electron-transfer rate constants for the donor-

Table 3. Charge-Transfer Complexes of Olefins with Various Acceptors^a

olefin donor	acceptor ^b	ΔG_0^c (eV)	k_{ET}^d (s ⁻¹)
2,3-dimethyl-2-butene	PMDA	-2.12	3.1×10^{11}
	TCNB	-2.28	1.2×10^{11}
	TCPA	-2.43	1.2×10^{11}
2,5-dimethyl-2-hexene	TCNE	-1.51	4.9×10^{11}
	PMDA	-2.30	1.9×10^{11}
	TCNB	-2.46	4.5×10^{10}

^a In dichloromethane solution at 25 °C. ^b PMDA = pyromellitic dianhydride, TCNB = tetracyanobenzene, TCPA = tetrachlorophthalic anhydride, TCNE = tetracyanoethylene. ^c Free-energy change calculated from the difference between the oxidation potential of the olefin donor and the reduction potential of the acceptor; taking $E^\circ(\text{TCNE}) = +0.24$ V,¹⁹ $E^\circ(\text{PMDA}) = -0.55$ V,^{48b} $E^\circ(\text{TCNB}) = -0.71$ V,^{37b} $E^\circ(\text{TCPA}) = -0.86$ V,^{48b} $E^\circ(2,3\text{-dimethyl-2-butene}) = +1.57$ V,⁵⁴ and $E^\circ(2,5\text{-dimethyl-2-hexene}) = +1.75$ V (interpolated from a plot of olefin oxidation potentials versus ionization potentials⁴⁹). [All potentials are given versus SCE.] ^d Rate constants for electron transfer following CT excitation of the complexes at 375 or 400 nm.

Table 4. Arene Complexes with Tetracyanobenzene^a or Methylviologen^b

arene donor	IP (eV)	acceptor ^c	k_{ET}^d (s ⁻¹)
toluene	8.8 ^e	MV	6.0×10^{10}
<i>p</i> -xylene	8.44 ^e	MV	7.7×10^{10}
durene	8.05 ^e	MV	2.4×10^{11}
pentamethylbenzene	7.92 ^e	MV	3.2×10^{11}
<i>p</i> -xylene	8.44 ^e	TCNB	9.3×10^8
durene	8.05 ^e	TCNB	2.0×10^9
hexamethylbenzene	7.85 ^e	TCNB	5.7×10^9
biphenyl	8.27 ^f	TCNB	2.0×10^8
2,6-dimethylnaphthalene	7.78 ^g	TCNB	2.1×10^9
anthracene	7.43 ^h	TCNB	7.9×10^9
9-methylanthracene	7.25 ^h	TCNB	1.2×10^{10}
9,10-dimethylanthracene	7.11 ^h	TCNB	1.5×10^{10}

^a In dichloromethane at 25 °C. ^b In acetonitrile. ^c MV = methylviologen, TCNB = 1,2,4,5-tetracyanobenzene. ^d Rate constants of electron transfer following the CT excitation of the complex at 375 or 400 nm. ^e Reference 48a. ^f Reference 46b. ^g Reference 21d. ^h Reference 50a.

acceptor combinations listed in Table 4 were either taken from earlier work³⁶ or measured for this study with standard pump-probe techniques using either the picosecond (Nd:YAG) or the femtosecond (Ti:sapphire) time-resolved spectrometer (see the Experimental Section).

Discussion

The striking result of this study is the observation of nonvariant electron-transfer rate constants (k_{ET}) following photoexcitation of various olefin complexes of TCNE, as listed in Table 1. Figure 4 illustrates the correlation of $\ln k_{\text{ET}}$ versus the electron-transfer driving force, as evaluated by the ionization potential of the olefin. Over a driving-force range of about 1 eV, the data points (triangles in Figure 4) are randomly scattered about the average rate constant of $k_{\text{ET}} = (4.6 \pm 0.9) \times 10^{11} \text{ s}^{-1}$ (horizontal line). In contrast, the fitted line of the corresponding data on arene/TCNE complexes (full circles in Figure 4) shows a negative slope of 2.75 eV^{-1} . Similarly, the electron-transfer rate constants obtained from olefin complexes with aromatic acceptors varied significantly with the ET driving force as demonstrated in Table 3. Thus, the remarkable effect of nonvariant electron-transfer rates over quite a large range of driving force is restricted to the olefin/TCNE charge-transfer complexes, which represent the unique combination of the smallest π -donors with a very compact and powerful π -acceptor.

I. Radical-Ion Pairs from CT Excitation vs ET Quenching. The radical-ion pairs generated via charge-transfer excita-

(35) (a) An alternative pathway for the collapse of the [olefin^{•+}, TCNE^{•-}] ion pair would be formation of a biradical by bond formation between the cation and anion. This reaction would lead to the formation of cyclobutane photoproducts and would be characterized by incomplete recovery of the ground-state EDA complex. In the case of the biphenyl/TCNE complex, we observed the complete recovery of the bleach of the CT absorption band at the same rate as the concomitant decay of the absorption bands of biphenyl cation radical and TCNE anion radical. In the case of the olefin/TCNE complexes, the direct monitoring of the bleach and recovery of the CT absorption bands was not possible because of the spectral overlap of these bands with the absorption band of TCNE^{•-}. (See Table 1 and Figure 2.) Thus, photoproduct studies on the steady-state time scale were carried out to probe the possible involvement of biradical intermediates. No photoconversion of the olefin norbornene or 2-hexene was observed even after prolonged (20 h) 366-nm photolysis of the corresponding TCNE complexes in dichloromethane. Photochemical quantum yields of less than 0.03 for the photoconversion of the olefins were estimated on the basis of the error limits ($\pm 5\%$) of the GC analysis. Since the singlet^{35d} biradicals formed by collapse of the ion pairs are expected to undergo efficient ring closure to cyclobutanes,^{35b,c} we conclude that biradical formation is at most a minor pathway in the decay of the olefin/TCNE ion pairs in Table 1. However, there are indications that biradical intermediates may be formed by collapse of the contact ion pair in the triplet manifold.^{35b,c} (b) Erickson, J. A.; Kahn, S. D. *Tetrahedron* **1993**, *49*, 9699. (c) Eckert, G.; Goetz, M. *J. Am. Chem. Soc.* **1994**, *116*, 11999. (d) The high ("optimized") rate constants for electron transfer in eq 4 suggest that the CT ion pairs [olefin^{•+}, TCNE^{•-}] remain in the singlet manifold throughout the decay process to the spectral baseline. Intersystem crossing to the triplet manifold is too slow to compete^{35e,f} with this fast collapse and would also generate long-lived ($> 10 \mu\text{s}$) triplet radical-ion pairs,⁷⁵ which are not observed. (e) Orbach, N.; Ottolenghi, M. In ref 73, p 75. (f) Ottolenghi, M. *Acc. Chem. Res.* **1973**, *6*, 153 and references therein.

(36) Hubig, S. M.; Kochi, J. K. *J. Phys. Chem.* **1995**, *99*, 17578.

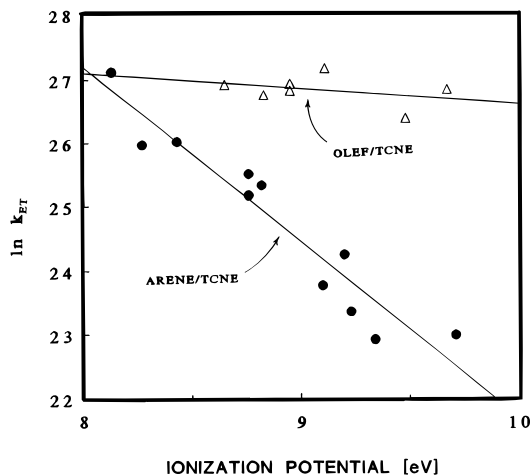
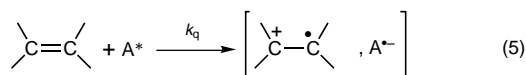


Figure 4. Free-energy correlation of electron-transfer rates ($\ln k_{ET}$) in dichloromethane at 25 °C versus the ionization potential of olefin (Δ) and arene (\bullet) donors.

tion of the EDA complexes according to eq 2 are to be compared with the radical-ion pairs derived by the more conventional process involving the quenching of a photoexcited acceptor, A^* , e.g.



where A represents cyanoarenes, quinones, TCNE, etc.^{4–8,37}

a. CT Excitation. Photoexcitation of the EDA complexes generates charge-transfer ion pairs that collapse by electron transfer from the anion to the cation radical. As a result, the ground-state EDA complex is completely restored (eq 4).³⁷ It has been shown for various combinations of electron donors and acceptors^{9–13} that the ET rates in charge-transfer ion pairs do not follow the bell-shaped correlation of $\ln k_{ET}$ versus the driving force ΔG_0 , as predicted by Marcus theory.³⁸ Instead, a simple linear energy-gap law relating $\ln k_{ET}$ and ΔG_0 has been proposed by Mataga and Asahi,^{9–13} i.e.

$$\ln k_{ET} = \alpha - \beta |\Delta G_0'| \quad (6)$$

where the driving force $\Delta G_0'$ is calculated from the difference between the oxidation potential of the electron donor and the reduction potential of the acceptor, corrected for solvation energy and Coulombic work terms.¹³ The slopes (β) have been determined in various homogeneous^{10–13} and heterogeneous^{36,39} environments—with the compelling result that similar β -values ($2–3 \text{ eV}^{-1}$) are obtained for all charge-transfer ion pairs. For instance, for the EDA complexes of arene donors with various acid anhydrides as acceptors, a β -value of 2.8 eV^{-1} was reported to be independent of the solvent (acetonitrile, ethyl acetate, and acetone).¹³

(37) (a) It is commonly accepted^{37bc} that the thorough analysis of the comparative behavior of ion pairs generated *via* charge-transfer excitation and *via* electron-transfer quenching is essential for a complete understanding of electron-transfer dynamics. (b) Ojima, S.; Miyasaka, H.; Mataga, N. *J. Phys. Chem.* **1990**, *94*, 4147, 5834, 7534. (c) See also refs 9–13. (d) Note that the ion-pair separation processes described in ref 37b do not pertain to the excited TCNE complexes, since the ion-pair collapse in eq 4 occurs with unit efficiency on the picosecond time scale. No absorption of the separated ions was observed (see the Experimental Section).

(38) Marcus, R. A.; Sutin, N. *Biochim. Biophys. Acta* **1985**, *811*, 265.

(39) (a) Miyasaka, H.; Kotani, S.; Itaya, A. *J. Phys. Chem.* **1995**, *99*, 5757. (b) Hubig, S. M. *J. Phys. Chem.* **1992**, *96*, 2903.

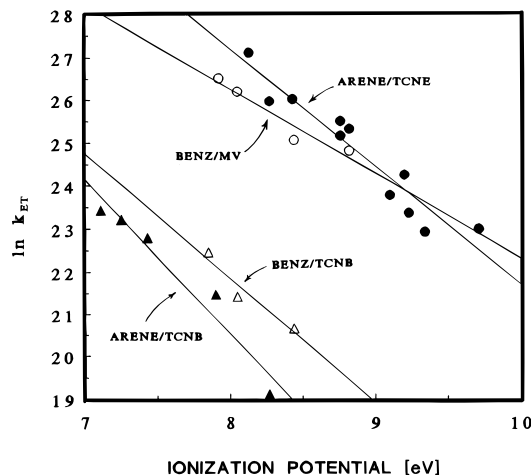


Figure 5. Free-energy correlation of electron-transfer rates ($\ln k_{ET}$) versus the ionization potentials of benzene (BENZ) and arene (ARENE) donors (as indicated) from Tables 2 and 4.

In accord with these previous observations, we examined various types of EDA complexes, with regard to β -values, as shown in Chart 1. The results in Chart 1 are illustrated in Figures 4 and 5, and they confirm the general applicability of eq 6. The olefin/TCNE complexes represent the sole example with a β -value of zero.⁴⁰ Interestingly, the donors consisting

Chart 1. Variation in the β -Parameter for Various EDA Complexes, As Evaluated from the Energy-Gap Law in Eq 6

	EDA complex	solvent	β (eV^{-1})
(a)	[benzenes, TCNB]	CH_2Cl_2	2.9
(b)	[larger aromatics, TCNB]	CH_2Cl_2	3.6
(c)	[benzenes, methylviologen]	CH_3CN	2.0
(d)	[benzenes, TCNE]	CH_2Cl_2	2.8
(e)	[olefins, TCNE]	CH_2Cl_2	0.0

of an aromatic and an olefinic π -system, either in conjugation (e.g., styrene or indene) or separated (e.g., allylbenzene), showed ET rate constants that varied with the driving force in the same way as those observed for the simple arene donors. [Note that the data points for styrene, indene, and allylbenzene fit well on the arene/TCNE correlation in Figure 4.]

b. ET Quenching. Radical-ion pairs generated by ET quenching of excited acceptors (eq 5) show a very different driving-force dependence of the electron-transfer rates. In this case, plots of $\log k_{ET}$ versus ΔG_0 show a characteristic (bell-shaped) curvature that can best be fitted using the correlation in eq 7, as originally formulated for nonadiabatic electron transfer.⁴¹ This free-energy relationship is based on a semiclassical model that considers various rate-controlling parameters including the electron exchange matrix element (ξ) between electron donor and acceptor, the solvent reorganization energy (λ_s), the internal reorganization energy (λ_i) and the electron-

(40) (a) The slight slope of the linear fit ($\beta = 0.2$) is negligible compared to the error limits ($\pm 20\%$) of the kinetic measurements. (b) In the case of benzene/TCNB complexes (see entry a in Chart 1), the data were operationally fitted to a straight line, although some curvature in the data points was apparent (see Figure 5).

(41) (a) Equation 7 is a variation of the original quadratic Marcus equation³⁸ taking into account less curved correlations in the highly exergonic region.^{55,56} (b) Note that the value of S itself depends on λ_i and the mean vibrational energy (σ) of the donor and the acceptor involved in the electron-transfer process. (c) A variety of symbols for the electron exchange matrix element, such as V ,^{4–8} H_{AB} ,³⁴ J ,¹⁷ B ,⁵² etc., have been introduced, each indicative of a particular theoretical perspective. Accordingly, we choose ξ as an unbiased (operational) designation to avoid confinement to a particular theoretical viewpoint.

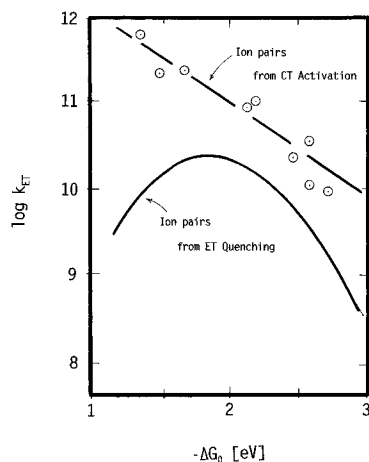


Figure 6. Bell-shaped free-energy relationship of electron-transfer rates ($\log k_{\text{ET}}$) from quenching studies of various arene donors with (excited) 9,10-dicyanoanthracene in acetonitrile from ref 5. The data points represent our electron-transfer rates obtained from the CT excitation of TCNE complexes of arene donors as listed in Table 2.

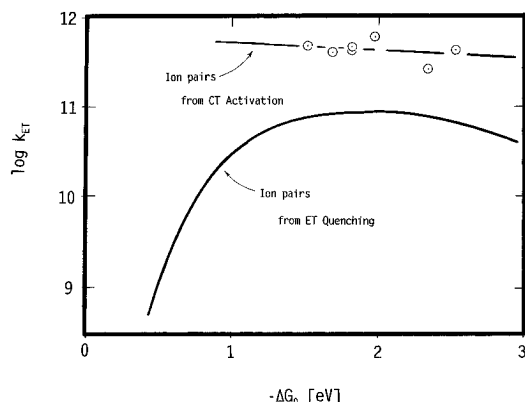


Figure 7. Flattened (bell-shaped) free-energy relationship of electron-transfer rates ($\log k_{\text{ET}}$) from quenching studies of various olefin donors with (excited) 9,10-dicyanoanthracene in acetonitrile from ref 6. The data points represent our electron-transfer rates obtained from the CT excitation of TCNE complexes of olefin donors as listed in Table 1.

vibration coupling constant S .⁴¹ The nonadiabatic formulation for electron transfer is given as

$$k_{\text{ET}} = (4\pi^2/h)\xi^2 \sum_j (e^{-S} S^j / j!) (4\pi\lambda_S k_B T)^{-1/2} \times \exp\left[-\frac{(j\sigma + \Delta G_0 + \lambda_S)^2}{4\lambda_S k_B T}\right] \quad (7)$$

where $S = \lambda_i/\sigma$ and the summation (j) is carried out over all of the vibrational modes of the donor and acceptor. Notably, eq 7 has served as the basis for several successful treatments of electron-transfer quenching data.⁴⁻⁸

II. New Trends in Electron-Transfer Rates of Radical-Ion Pairs. The use of the nonadiabatic electron-transfer formulation (eq 7) allows the generation of bell-shaped curves with various widths and symmetries, as shown in Figures 6 and 7. The flatness and symmetry of these curves are particularly dependent on the parameters S and σ .⁶ To generate the bell-shaped ($\log k_{\text{ET}}$ versus ΔG_0) correlation in Figure 6, we used the fitting parameters that were obtained from quenching experiments of excited dicyanoanthracene (DCA)⁴² with various benzene derivatives.⁵ It is evident that our data, obtained from CT excitation of arene/TCNE complexes (full circles), do not fit on the simulated curve derived from eq 7. Rather, they follow the separate linear correlation described by eq 6.

The ET rate constants of olefin complexes in Table 1 are even more difficult to reconcile with the bell-shaped free-energy relationship described by eq 7. Thus, Figure 7 illustrates a comparison of our data on olefin/TCNE charge-transfer ion pairs with the DCA quenching data involving olefins,⁴² as previously measured by Haselbach and co-workers.⁶ The bell-shaped curve is simulated using eq 7 with the fitting parameters obtained from ET quenching.⁶ The mild curvature of the simulation in the region $-1.5 \text{ eV} > \Delta G_0 > -2.5 \text{ eV}$, as compared to the much stronger curved simulation in Figure 6, is achieved by choosing a relatively high reorganization energy ($\lambda = \lambda_i + \lambda_S = 2.1 \text{ eV}$) and a vibrational energy ($\sigma = 0.484 \text{ eV}$) which is 3 times as high as the one commonly used for aromatic donors.⁶ The high λ value was obtained by a substantial increase in the internal reorganization energy ($\lambda_i = 1.1 \text{ eV}$).⁶ Accompanying the bell-shaped curve in Figure 7 are our data obtained from CT excitation of olefin/TCNE complexes.

In order to reconcile the opposed trends in both Figures 6 and 7, let us consider various approaches to linearize the free-energy relationship by (a) the manipulation of λ_i and σ in eq 7, (b) the assignment of unique values of λ_S to each of the donors in Figure 7, or (c) the generation of a new free-energy relationship and variation of ξ .

Approach a. The bell-shaped free-energy relationship typically illustrated in Figure 6 can be altered to the flattened curve in Figure 7 by increasing the variable parameters λ_i and σ in eq 7. The flatness of the simulated curve in Figure 7 suggests that, by further manipulation of λ_i and σ , a quasi-linear correlation may be obtained that approximates our data on olefin/TCNE complexes.

Approach b. An alternative approach for a linear simulation as observed in CT excitation experiments⁹⁻¹³ has been recently suggested for contact ion pairs on the basis of the electron-transfer model of eq 7, combined with a continuous change of λ_S accompanying the change in the driving force ΔG_0 .¹⁶ Thus, in the case of benzene/TCNB complexes, a linear correlation between $\log k_{\text{ET}}$ and ΔG_0 could be simulated under the condition that a λ_S -shift of 250 meV accompanied the ΔG_0 change of 600 meV from hexamethylbenzene to xylene.^{43a} Such a shift in λ_S may also explain our linear data on olefin/TCNE complexes displayed in Figure 7. In this case, however, the solvent reorganization energy must be shifted by as much as 1 eV to simulate a nonvariant electron-transfer rate over the observed range of driving force in Figure 7.^{43b}

Approach c. The conventional Marcus equation³⁸ can be modified in a way that the variation of the electron exchange matrix element (ξ) between the donor and the acceptor controls the shape of the simulated curve substantially. Thus, by varying ξ between 0 and 0.3 eV, Tachiya and Murata were able to fit

(42) Our attempts to excite tetracyanoethylene (with the 266-nm output of a Q-switched Nd:YAG laser) and to study the subsequent electron-transfer quenching of the excited TCNE* with olefin donors were uniformly unsuccessful. No transient absorption (of TCNE*, TCNE⁻, or of any other species) was observed. The lifetime of the photoexcited TCNE was evidently too short (<100 ps) to be diffusionally quenched by donors even when they were present at high (ca. 1 M) concentrations.

(43) (a) This remarkable shift in λ_S was experimentally justified on the basis of a careful analysis of CT absorption and emission data.¹⁶ (b) In nonpolar solvents (e.g., dichloromethane) pertinent to this study, such a large change in the solvent reorganization energy is difficult to justify in view of the limited values of λ_S which pertain to nonpolar solvents.⁷² (c) However, changes in λ_i by as much as 1 eV (upon change of the substitution on the double bond) may be possible for olefinic donors, owing to their small size. These changes may be separately evaluated by a detailed analysis of the charge-transfer absorption bands according to the Hush model.^{43d,e} We thank a reviewer for this helpful suggestion. (d) Hush, N. S. *Prog. Inorg. Chem.* **1967**, *8*, 391. (e) Benniston, A. C.; Harriman, A. *J. Am. Chem. Soc.* **1994**, *116*, 11531.

both the bell-shaped ET quenching and the linear CT excitation data with the same equation.¹⁷

All three theoretical approaches to simulate the linear or quasi-linear correlations of $\log k_{\text{ET}}$ versus ΔG_0 are based on modifications of the original outer-sphere electron-transfer model. Such alterations of the fitting parameters necessarily raise questions about the chemical significance of these manipulations. For instance, how can a high internal reorganization energy and an extraordinary vibrational energy, as in approach a, be explained in terms of electronic and structural properties of the radical-ion pair from the olefin complex? What chemical criterion can be invoked in approach b to justify a 1-eV shift in either λ_i or λ_s for charge-transfer ion pairs involving olefin donors?^{243b,c} Furthermore, what chemical meaning can be attached to the manipulation of ξ in approach c?

To address these questions, let us consider the above methods to simulate linear or quasi-linear correlations of $\log k_{\text{ET}}$ versus ΔG_0 as representing attempts to integrate inner-sphere processes into a purely outer-sphere electron-transfer model. For example, the attempt to fit inner-sphere electron-transfer processes to an outer-sphere model in approaches a and b will yield values of $\lambda = \lambda_i + \lambda_s$ that are both large and substrate-dependent, owing to the extensive changes in structure, electronic configuration, and solvation that attend the formation of the donor-acceptor "bonded" transition state. The alternative approach c of increasing the value of the electron exchange matrix ξ directly invokes bonding within the radical-ion pair in eq 4.⁴⁴ Thus, all three approaches implicitly invoke bonding (orbital overlap) of the donor and acceptor in the charge-transfer ion pair.

III. Inner-Sphere and Outer-Sphere Mechanisms for Electron Transfer. The existence of a significant bonding interaction between donor and acceptor within the contact ion pair implies that electron transfer must proceed by an inner-sphere mechanism. The term "inner-sphere" was originally applied to electron transfer between inorganic redox centers connected by a bridging ligand.⁴⁵ Its meaning has been extended to encompass electron transfer between (inorganic or organic) donors and acceptors that are strongly coupled due to the mutual interpenetration of their coordination spheres.⁵¹⁻⁵⁴ The coordinatively saturated character of organic compounds has hampered the consideration of inner-sphere mechanisms since the donor and the acceptor molecules cannot be joined

by a conventional two-electron bond as described by valence-bond theory. However, the introduction of molecular orbitals allows for a description of bonding³⁴ between the donor (HOMO) and the acceptor (LUMO) within the charge-transfer ion pair to a degree that justifies the consideration of an inner-sphere electron transfer. Such a description may be contrasted with the more conventional outer-sphere mechanism as follows.

Outer-sphere electron transfer occurs between minimally interacting electron donors and acceptors, and it is successfully treated by the various formulations of Marcus theory.^{38,55,56} In the outer-sphere model, the electron is transferred nonadiabatically by tunneling from the potential energy surface of the donor to that of the acceptor.⁵⁷ As we have seen in Figures 6 and 7 (see curved simulations), electron transfer in ion pairs generated by ET quenching represents a notably successful application of the outer-sphere approach.

Inner-sphere electron transfer, on the other hand, proceeds from strongly coupled donors and acceptors. In this mechanism, electron transfer occurs adiabatically by an avoided crossing of donor and acceptor potential energy surfaces.⁵⁷ A theory for the inner-sphere (adiabatic) electron transfer is presently in a stage of active development.⁵⁸ Significant inner-sphere components in electron-transfer processes have been revealed previously for reactions between various organometal donors and TCNE,⁵³ and for the bromination and mercuration reactions of olefins.⁵⁴ The excitation of EDA complexes, in particular, generates donors and acceptors which undergo electron transfer by way of the inner-sphere mechanism.⁵⁹ Three effects signal the involvement of pronounced inner-sphere processes, namely, (i) electron-transfer rates that are faster than predicted on the basis of the outer-sphere model,^{52,54} (ii) a driving-force dependence that deviates significantly from that predicted by Marcus theory,^{51,53,54} and (iii) pronounced steric effects on the electron-transfer rates.⁵⁴ The first two criteria are clearly demonstrated in the electron-transfer behavior of charge-transfer ion pairs derived from olefin/TCNE complexes (see Figure 7). The steric effect in charge-transfer ion pairs may be recognized in this study by the different electron-transfer behavior of olefins as compared to that of arenes (see Figure 4). We believe that the unique driving-force dependence observed with olefins can be attributed to the compact size and characteristic orientation of their π -orbitals as compared to the more delocalized aromatic π -systems. Thus, the highly localized charge and spin-density distribution in the olefin cation radical and the TCNE anion radical points to the possibility of "bond" formation. Chart 2 illustrates how the olefin cation radical and tetracyanoethylene anion radical can be intimately juxtaposed for optimum inner-sphere interaction. Despite this intimacy, the ion-radical components retain their integrity, as demonstrated by the unshifted/undistorted transient spectra of TCNE⁻ in Figures 2 and 3 that are identical (including the vibrational fine structure)

(44) The electron exchange matrix element, ξ , is analogous to the "Coulombic" integral, which expresses the bonding overlap between donor and acceptor in the radical-ion pair. See: Eyring, H.; Walter, J.; Kimball, G. E. *Quantum Chemistry*; Wiley: New York, 1948; p 149.

(45) (a) Taube, H.; Gould, E. S. *Acc. Chem. Res.* **1969**, *2*, 321. (b) Cannon, R. D. *Electron Transfer Reactions*; Butterworths: London, 1980. (c) Henderson, R. A. *The Mechanisms of Reactions at Transition Metal Sites*; Oxford University Press: New York, 1993; pp 46 f.

(46) (a) Nelson, D. J.; Cooper, P. J.; Soundararajan, R. *J. Am. Chem. Soc.* **1989**, *111*, 1414. (b) West, R. C., Ed. *CRC Handbook of Chemistry and Physics*; CRC Press: Boca Raton, FL, 1989.

(47) (a) Rosenstock, H. M.; Draxl, K.; Steiner, B. W.; Herron, J. T. *Energetics of Gaseous Ions*. *J. Phys. Chem. Ref. Data* **1977**, *6* (Suppl. 1). (b) Palmer, M. H.; Moyes, W.; Speirs, M. J. *Mol. Struct.* **1980**, *62*, 165.

(48) (a) Howell, J. O.; Goncalves, J. M.; Amatore, C.; Klasinc, L.; Wightman, R. M.; Kochi, J. K. *J. Am. Chem. Soc.* **1984**, *106*, 3968. (b) Bard, A. J.; Lund, H., Eds. *Encyclopedia of Electrochemistry of the Elements*, Organic Section; Marcel Dekker: New York, 1978; Vol. 12, p 263.

(49) Fleischmann, M.; Pletcher, D. *Tetrahedron Lett.* **1968**, *60*, 6255.

(50) (a) Masnovi, J. M.; Seddon, E. A.; Kochi, J. K. *Can. J. Chem.* **1984**, *62*, 2552. (b) Kimura, K.; Katsumata, S.; Achiba, Y.; Yamazaki, T.; Iwata, S. *Handbook of HeI Photoelectron Spectra of Fundamental Organic Molecules*; Halsted Press: New York, 1981.

(51) Kochi, J. K. *Angew. Chem., Int. Ed. Engl.* **1988**, *27*, 1227.

(52) (a) Ebersson, L.; Shaik, S. S. *J. Am. Chem. Soc.* **1990**, *112*, 4484. (b) See also ref 59.

(53) Fukuzumi, S.; Wong, C. L.; Kochi, J. K. *J. Am. Chem. Soc.* **1980**, *102*, 2928.

(54) Fukuzumi, S.; Kochi, J. K. *Bull. Chem. Soc. Jpn.* **1983**, *56*, 969.

(55) (a) Van Duyne, R. P.; Fischer, S. F. *Chem. Phys.* **1974**, *5*, 183. (b) Ulstrup, J.; Jortner, J. *J. Chem. Phys.* **1975**, *63*, 4358.

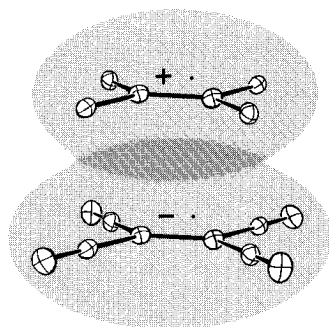
(56) Miller, J. R.; Beitz, J. V.; Huddleston, R. K. *J. Am. Chem. Soc.* **1984**, *106*, 5057.

(57) Bolton, J. R.; Archer, M. D. In *Electron Transfer in Inorganic, Organic, and Biological Systems*; Bolton, J. R., Mataga, N., McLendon, G., Eds.; American Chemical Society: Washington, DC, 1991; p 7.

(58) (a) Lindenberg, K.; Cortes, E.; Pearlstein, R. M. *J. Phys. Chem.* **1994**, *98*, 7395. (b) Stuchebrukhov, A. A.; Song, X. *J. Chem. Phys.* **1994**, *101*, 9354. (c) Dakhnovskii, Y. L.; Doolen, R.; Simon, J. D. *J. Chem. Phys.* **1994**, *101*, 6640. (d) Zharikov, A. A.; Frantsuzov, P. A. *Chem. Phys. Lett.* **1994**, *220*, 319. (e) Liu, Y.-P.; Newton, M. D. *J. Phys. Chem.* **1995**, *99*, 12382.

(59) (a) Inner-sphere effects have been definitively established for the excited arene/nitrosonium^{59b} and arene/bromine atom^{59c} complexes. (b) Bockman, T. M.; Karpinski, Z. J.; Sankararaman, S.; Kochi, J. K. *J. Am. Chem. Soc.* **1992**, *114*, 1970. (c) Hörmann, A.; Jarzaba, W.; Barbara, P. F. *J. Phys. Chem.* **1995**, *99*, 2006.

Chart 2. Charge-Transfer Model of the Contact Ion Pair Depicting the Mutual Interpenetration of the Coordination Spheres of the Olefin Cation and the Tetracyanoethylene Anion According to the Inner-Sphere Formulation



to previously reported spectra of $\text{TCNE}^{\bullet-}$ in its various isolated forms.³¹ Indeed, *ab initio* calculations confirm the incipient bonding in the related ethylene cation-radical complex.¹⁸ In this context, the consideration of inner-sphere components in electron-transfer reactions with olefins will support the generally accepted concept that the crucial step in ET-sensitized [2+2] cycloadditions (e.g., styrene dimerization) is the σ -bond formation between the olefinic cation radical and the parent olefin.⁶⁰ Moreover, the polar mechanism as generally suggested for electrophilic additions of olefins with TCNE⁶¹ may be closely related to inner-sphere electron transfer, since both mechanisms invoke partial bonding in the transition state.

Partial bonding between donors and acceptors was originally proposed by Mulliken to account for the varying stability of ground-state EDA complexes.³⁴ For neutral species, van der Waals forces play a dominant role and charge-transfer interactions are usually minor contributors to the stability of the complex.⁶² In other instances, hydrogen bonding or Coulombic forces predominate.⁶³ In some cases, such as the EDA complexes of nitrosonium (NO^+) with aromatic donors⁶⁴ or the EDA complexes of carbon tetrabromide with amine donors,⁶⁵ stronger (*quasi*-covalent) bonds are invoked.⁶⁶ For olefins, σ -bonds are postulated for the inner-sphere complexes with silver(I) which accept electrons from the bonding 2p π -orbital of the olefin.⁶⁷ Moreover, strong back-donation in complexes of TCNE with transition metals such as $(\eta^2\text{-TCNE})\text{Cr}(\text{CO})_5$ confirms the capability of olefins to carry out inner-sphere electron exchange through bond formation.⁶⁸

The incursion of inner-sphere (adiabatic) electron transfer reflects an increase in the electronic coupling (ξ) between donor

(60) Lewis, F. D. In *Photoinduced Electron Transfer*; Fox, M. A., Chanon, M., Eds.; Elsevier: Amsterdam, 1988; Part C, p 1 and references therein.

(61) Kim, T.; Sarker, H.; Bauld, N. L. *J. Chem. Soc., Perkin Trans. 2* **1995**, 577.

(62) Foster, R. *Organic Charge-Transfer Complexes*; Academic Press: New York, 1969.

(63) Denisov, G. S.; Bureiko, S. F.; Golubev, N. S.; Tokhadze, K. G. In *Molecular Interactions*; Ratajczak, H., Orville-Thomas, W. J., Redshaw, M., Eds.; Wiley: New York, 1981; Vol. 2, p 107.

(64) Kim, E. K.; Kochi, J. K. *J. Am. Chem. Soc.* **1991**, *113*, 4962. See also ref 59.

(65) (a) Blackstock, S. C.; Lorand, J. P.; Kochi, J. K. *J. Org. Chem.* **1987**, *52*, 1451. (b) Blackstock, S. C.; Kochi, J. K. *J. Am. Chem. Soc.* **1987**, *109*, 2484.

(66) The consideration of *quasi*-covalent bonds is based on the observation of close donor-acceptor distances as revealed by X-ray crystallography of CT crystals.^{64,65} In addition, red-shifted IR (stretch) frequencies in the EDA complexes as compared to the single components indicate bond formation between the donor and acceptor moieties.⁶⁴

(67) Beverwijk, C. D.; van der Kerk, G. M. J.; Leusink, A. J.; Noltes, J. G.; *Organomet. Chem. Rev.* **1970**, *A5*, 215.

(68) Kaim, W.; Olbrich-Deussner, B.; Roth, T. *Organometallics* **1991**, *10*, 410.

and acceptor. Although the consequences of electron transfer in the strong coupling limit have not yet been placed on a sound theoretical basis, it is possible that electron transfer within a strongly interacting donor-acceptor (D-A) pair may become independent of the thermodynamic driving force.⁶⁹ For the inner-sphere (adiabatic) situation, it is important to realize that the conventional parameters λ_i and λ_S will not have the meaning that is assigned to them in the nonadiabatic electron-transfer model.⁷⁰ Thus, one signal which would indicate that the inner-sphere process is operating would be values of λ_i and λ_S that are unusually large or are not consistent with conventional nonadiabatic calculations.⁷¹

Electronic coupling in inner-sphere ion pairs implies charge delocalization between the cationic and anionic moieties. Thus, mixing between [D, A] and $[\text{D}^{\bullet+}, \text{A}^{\bullet-}]$ states occurs in the ion-pair state, as suggested for the electronic ground state of EDA complexes.³⁴ In addition, locally excited configurations, such as $[\text{D}^*, \text{A}]$ or $[\text{D}, \text{A}^*]$, will also contribute if their energies are close to those of the ion pair $[\text{D}^{\bullet+}, \text{A}^{\bullet-}]$. The resulting entity, described by a three-state model,⁷² is an exciplex.⁷³ Exciplexes have been established by emission and absorption spectroscopy as intermediates in various ET quenching experiments involving singlet⁷⁴ and triplet⁷⁵ excited states, and the close relationship between exciplexes and excited charge-transfer complexes has been explicitly addressed.^{72,76} Moreover, the bonding interaction between donors and acceptors within the exciplex, i.e., a combination of van der Waals forces, hydrogen bonding, Coulombic interactions, etc., is of the same nature as that within the EDA complexes.⁷⁷ Accordingly, the inner-sphere model is particularly applicable to electron transfer within the exciplex, and exciplexes thus represent a special case of inner-sphere ion pairs.

Summary and Conclusions

By considering the variety of inner-sphere electron-transfer reactions reported for olefins, we can now understand the non-Marcus ET behavior of charge-transfer ion pairs from olefin/TCNE complexes. The nonvariant electron-transfer rate observed here is the extreme case of the linear $\log k_{\text{ET}}$ versus ΔG_0

(69) Yoshihara, K.; Tominaga, K.; Nagasawa, Y. *Bull. Chem. Soc. Jpn.* **1995**, *68*, 696.

(70) Rauhut, G.; Clark, T. *J. Am. Chem. Soc.* **1993**, *115*, 9127.

(71) For example, the reorganization energy $\lambda = \lambda_i + \lambda_S$ derived from the spectral analysis^{43d} of the charge-transfer bands of the olefin/TCNE complexes was approximately 1 eV. This value of λ does not agree with the value of $\lambda_i + \lambda_S = 2.1$ eV obtained from electron-transfer rate constants.⁶

(72) (a) Gould, I. R.; Young, R. H.; Mueller, L. J.; Farid, S. *J. Am. Chem. Soc.* **1994**, *116*, 8176. (b) Gould, I. R.; Young, R. H.; Mueller, L. J.; Albrecht, A. C.; Farid, S. *J. Am. Chem. Soc.* **1994**, *116*, 8188.

(73) Gordon, M., Ware, W. R., Eds. *The Exciplex*; Academic: New York, 1975.

(74) (a) Mataga, N.; Okada, T.; Yamamoto, N. *Bull. Chem. Soc. Jpn.* **1966**, *39*, 2562. (b) Knibbe, H.; Rehm, D.; Weller, A. *Ber. Bunsen-Ges. Phys. Chem.* **1968**, *72*, 257. (c) Itoh, M.; Furuya, S.-I.; Okamoto, T. *Bull. Chem. Soc. Jpn.* **1977**, *50*, 2509. (d) Weller, A. *Z. Phys. Chem. N. F.* **1982**, *133*, 93. (e) Kuzmin, M. G. *Pure Appl. Chem.* **1993**, *65*, 1653. (f) Chakraborty, T.; Sun, S.; Lim, E. C. *J. Am. Chem. Soc.* **1994**, *116*, 10050.

(75) (a) Kobashi, H.; Funabashi, M.-A.; Kondo, T.; Morita, T.; Okada, T.; Mataga, N. *Bull. Chem. Soc. Jpn.* **1984**, *57*, 3557. (b) Levin, P. P.; Kuzmin, V. A. *Russ. Chem. Rev.* **1987**, *56*, 307. (c) Jones, G., II; Mouli, N. *J. Phys. Chem.* **1988**, *92*, 7174. (d) Levin, P. P.; Raghavan, P. K. N. *Chem. Phys. Lett.* **1991**, *182*, 663. (e) Tahara, T.; Hamaguchi, H.-O. *J. Phys. Chem.* **1992**, *96*, 8252.

(76) In the case of the charge-transfer excitation of EDA complexes of olefins with TCNE, the role of locally excited states is unclear, since the first excited singlet states of both the donor and acceptor are high-energy states, which are unlikely to mix with the $[\text{olefin}^{\bullet+}, \text{TCNE}^{\bullet-}]$ ion-pair state. There is no evidence for exciplex formation in the transient absorption spectra of the ion pairs, since only the undistorted 450-nm band of $\text{TCNE}^{\bullet-}$ is observed.

(77) (a) Anner, O.; Haas, Y. *J. Am. Chem. Soc.* **1988**, *110*, 1416. (b) Förster, T. In ref 73, p 1. (c) Mataga, N. In ref 73, p 113.

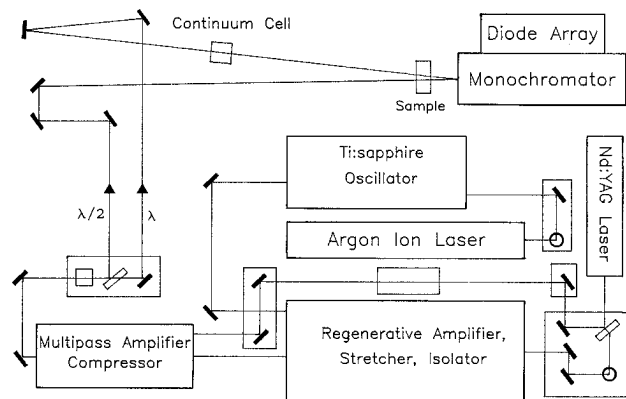


Figure 8. General layout of the femtosecond Ti:sapphire laser system.

correlations with mild slopes that are commonly observed with other charge-transfer ion pairs involving aromatic molecules. It demonstrates that inner-sphere processes in charge-transfer ion pairs are most pronounced with olefin donors. Thus, we believe that electron-transfer studies with olefin charge-transfer ion pairs will be the proving ground to test new electron-transfer theories that explicitly consider the continuum of inner-sphere and outer-sphere processes.⁵³ In addition, the nonvariance of electron-transfer rates in olefin complexes serves to highlight the importance of steric effects in electron-transfer reactions.^{78a} We are currently examining such effects of steric "crowding" within ion pairs generated either by charge-transfer excitation or by electron-transfer quenching experiments.^{78b}

Experimental Section

Materials. Norbornene, 3,3-dimethyl-1-butene, 1-hexene, 2,3-dimethyl-1-butene, 2-hexene, 2,4,4-trimethyl-2-pentene, and 2,5-dimethyl-2-hexene from Aldrich or Wiley Chemicals were used as received. The arenes listed in Table 2 were available from a previous study.³⁶ Tetracyanoethylene (Aldrich) was further purified by sublimation *in vacuo*. Dichloromethane (Fisher) was repeatedly stirred with fresh aliquots of sulfuric acid (25% by volume) until the acid layer remained clear. The solvent was separated, and then washed sequentially with water, aqueous bicarbonate, water, and aqueous sodium chloride. After drying over calcium chloride, the dichloromethane was refluxed over P₂O₅ for 2 h, and distilled under a flow of argon. Acetonitrile (Fisher) was stirred over KMnO₄ for 24 h, and then refluxed for 1 h. The solid was filtered, and the clear solvent was distilled from phosphorous pentoxide under a flow of argon. The distillate was finally refluxed over calcium hydride for 6 h and then distilled under an argon atmosphere. Each purified solvent was stored in a Schlenk flask fitted with a Teflon stopcock.

Instrumentation. The UV-vis absorption spectra were recorded on a Hewlett-Packard 8450A diode-array spectrometer using a custom-made quartz cuvette fitted with a side arm and Teflon stopcock.

The time-resolved (femtosecond) spectrometer was constructed in conjunction with Photonics Industries, and the basic layout is shown in Figure 8. The heart of the system was a Ti:sapphire oscillator (Photonics Industries, TFO-100) which was pumped by an argon ion laser (Coherent, Innova-310). The design of the triple-folded cavity was based on the self-focusing and self-mode-locking properties of the Ti:sapphire crystal, which allowed the generation of 114-fs pulses ("true" pulse width corrected for hyperbolic secant pulse shape) with a repetition rate of about 79 MHz. Using two sets of optics, mode-locked pulses with a tuning range from below 720 to 920 nm and energies of about 5 nJ/pulse were obtained by applying pump energies of about 6 W, and harvesting mostly the 488- and 514-nm argon ion laser lines. Typically, bandwidths (fwhm) of about 7 nm were obtained. The nanojoule Ti:sapphire oscillator pulses were first directed through an isolator (Optics For Research) to prevent feedback into the oscillator

cavity and then through a pulse stretcher unit (Photonics Industries) utilizing a holographic grating to chirp the pulse by a factor of about 2000. The chirped pulse was seeded into the folded cavity of a Ti:sapphire regenerative amplifier (Photonics Industries, TRA-50) which was pumped by a Q-switched Nd:YAG laser (Continuum, Surelite-I) with a 10-Hz repetition rate and a pump energy of about 10 mJ/pulse. The regenerative-amplifier pulses were dumped employing a Pockels cell (Medox Electro-Optics) operating in a double-pass configuration. The Pockels cell was switched twice with a controlled delay of a few tens of nanoseconds which allowed exact timing of the entry of the seed pulse into the regenerative-amplifier cavity relative to the exit of dumped amplified pulses out of the cavity. In general, the seed pulse stayed in the cavity for less than 10 round trips (ca. 90 ns) before being dumped. The wavelength of the regenerative amplifier was tuned with a wavelength selector. Energies of the dumped pulses varied between 1 and 2 mJ depending on the wavelength. The laser pulses leaving the regenerative amplifier were fed into a multipass Ti:sapphire amplifier (Photonics Industries) which was pumped by the same Q-switched Nd:YAG laser that pumped the regenerative amplifier. The pump energy (up to 120 mJ/pulse) was adjusted using a combination of a Glan laser beam-splitting polarizer and a half-wave plate. The Ti:sapphire pulses passed through the amplifier crystal four times, reaching energies of up to 20 mJ after the fourth pass. This highly amplified pulse was then directed through a beam expander and compressed using a holographic grating. The pulse width of the compressed pulse was measured to be about 200 fs (fwhm). Depending on the Ti:sapphire laser wavelength and the pump energy applied, energies as high as 11 mJ could be obtained for the compressed pulses, which corresponded to peak powers of about 55 GW. The compressed amplified laser pulses were first directed through a second-harmonic generator (Photonics Industries) equipped with an uncoated LBO crystal of 3-mm thickness (Castech-Phoenix). About 30% of the light was converted into the second harmonic frequency and separated from the residual fundamental wavelength by a dichroic mirror. Bandwidths (fwhm) of about 3 nm were obtained. The frequency-doubled pulses, which were used as excitation ("pump") light, traversed a variable (up to 4 ns) delay stage (Velmetex) before being directed onto the sample cuvette. The fundamental laser pulses were focussed onto a 1-cm quartz cuvette containing a 1:1 mixture of water and D₂O to generate femtosecond supercontinuum pulses⁷⁹ that covered a wide wavelength range from below 350 to above 800 nm. The white light pulses were collimated to a narrow beam by means of two lenses in a telescope-like configuration and split into two directions utilizing a neutral-density filter as a semitransparent mirror. The reflected beam was picked up by fiber optics and used as the reference light. The transmitted portion of the beam was directed through the sample cuvette overlapping with the frequency-doubled excitation beam in order to probe the excited species. This probe light was picked up by a second optical fiber. Both the reference and the sample optical fibers were fed into a flat-field spectrograph (Instruments S.A., HR320) to which an unintensified dual-diode array detector (Princeton Instruments, DDA-512) was attached. Thus, with each single laser pulse, two spectra (excited sample and reference) were recorded simultaneously and a transient absorption spectrum of the excited species could be computed on the basis of Lambert-Beer's law: $A(\lambda) = \log\{I_0(\lambda)/I(\lambda)\}$, where $A(\lambda)$ is the transient absorbance at the wavelength λ and $I_0(\lambda)$ and $I(\lambda)$ are the intensities at the wavelength λ of the reference light and the sample light, respectively. In a typical experiment, 100 spectra were averaged and passed to a personal computer, *via* a Princeton Instruments interface, for data storage, display, and analysis. The overall time response of the pump-probe experiment was determined to be about 700 fs, as determined by monitoring the rise of 1,4-diphenylbutadiene and 1,8-diphenyloctatetraene singlet states for 375- and 400-nm excitation, respectively.⁸⁰

(79) Hubig, S. M.; Rodgers, M. A. J. In *Handbook of Organic Photochemistry*; Scaiano, J. C., Ed.; CRC Press: Boca Raton, FL, 1989; Vol. I, p 315.

(80) Goldbeck, R. A.; Twarowski, A. J.; Russell, E. L.; Rice, J. K.; Birge, R. R.; Switkes, E.; Klinger, D. S. *J. Chem. Phys.* **1982**, *77*, 3319.

(78) (a) Gould, I. R.; Farid, S. *J. Phys. Chem.* **1993**, *97*, 13067. (b) Rathore, R. Unpublished studies.

The companion time-resolved (picosecond) spectrometer based on a mode-locked Nd:YAG laser (Quantel YG501-C, 25 ps) was described previously.⁸¹

Photoexcitation of the EDA complexes of Tetracyanoethylene with Olefin and Arene Donors. For the laser photolysis experiments, solutions of tetracyanoethylene (0.02 M) and 0.5 M olefin or 0.3 M arene in dichloromethane were prepared. These donor and acceptor concentrations were chosen to ensure strong charge-transfer absorption (0.5–1.0 absorbance unit) at the laser-irradiation wavelength. The absorption spectra of the solutions were measured in a 0.5-cm quartz cuvette both before and after the laser experiment. No significant spectral changes due to the laser irradiation were observed. In a typical pump–probe experiment, 100–300 shots were averaged at a repetition rate of 10 Hz to obtain a complete transient spectrum for each delay time. The delay line was moved in 500-fs steps between the acquisition of each spectrum. Prior to each measurement the two diode arrays were balanced by acquiring 100–300 shots without laser excitation and correcting for the difference in the spectral response of the diodes. In all of the laser photolysis experiments, the transient absorbance decayed on the picosecond time scale to a zero baseline, and no long-lived residual components were observed. In all cases, the kinetic data could be fitted to a single exponential decay, with a satisfactory regression coefficient, and thus no evidence for nonexponential decay was found.^{33c}

Stoichiometry and Thermodynamics for the Charge-Transfer Ion Pairs. In the case of the photoexcited styrene/TCNE, indene/TCNE, and biphenyl/TCNE complexes, the transient spectra were analyzed as the sum of cation- and anion-radical absorptions and the bleaching (negative absorption) of the ground-state EDA complex. The absorption bands of the radical cations with absorption maxima at 620, 570, and 690 nm for styrene,⁸² indene,⁸³ and biphenyl,^{7a} respectively, as well as the absorption band of the tetracyanoethylene anion radical³¹ at 450 nm did not show any spectral distortion as compared with authentic spectra in the literature. In each case the experimental ratio of the absorption maxima for TCNE^{•-} and the aromatic cation radical was determined at 1 ps after excitation and compared with the theoretical ratio based on the extinction coefficients of TCNE^{•-}, the cation radical, and the CT absorption of the EDA complex.

For the biphenyl/TCNE complex in dichloromethane, the experimental ratio of the transient absorbances $A(450)/A(690)$ was measured to be 0.33. On the basis of $\epsilon_{450}(\text{TCNE}^{\bullet-}) = 5700 \text{ M}^{-1} \text{ cm}^{-1}$,^{31a} $\epsilon_{690}(\text{BIP}^{\bullet+}) = 9960 \text{ M}^{-1} \text{ cm}^{-1}$,^{7a} and $\epsilon_{450}(\text{EDA complex}) = 1900 \text{ M}^{-1} \text{ cm}^{-1}$,^{21c} a theoretical ratio of $(5700-1900)/9960 = 0.38$ was calculated assuming 1:1 cation/anion formation. The good agreement of the experimental and theoretical ratios confirmed the 1:1 stoichiometry in the formation of biphenyl cation radical and TCNE anion radical. The analogous analysis of the spectral bands recorded in acetonitrile yielded

(81) Yabe, T.; Kochi, J. K. *J. Am. Chem. Soc.* **1992**, *114*, 4491.

(82) Brede, O.; David, F.; Steenken, S. *J. Chem. Soc., Perkin Trans. 2* **1995**, 23.

(83) Bokin, A. I.; Petruschenka, K. B.; Turchaninov, V. K.; Gorshkov, A. G.; Nakhmanovich, A. S.; Domnina, E. S. *Z. Obshh. Khim. (Engl. Transl.)* **1988**, *58*, 905.

an experimental ratio $A(445)/A(680)$ of 0.73, in excellent agreement with the theoretical value of 0.71. For the indene/TCNE complex in dichloromethane, the experimental ratio $A(470)/A(600)$ was determined to be 1.6. On the basis of $\epsilon_{470}(\text{TCNE}^{\bullet-}) = 4300 \text{ M}^{-1} \text{ cm}^{-1}$,^{31a} $\epsilon_{600}(\text{IN}^{\bullet+}) = 2200 \text{ M}^{-1} \text{ cm}^{-1}$,⁸³ $\epsilon_{470}(\text{EDA complex}) = 640 \text{ M}^{-1} \text{ cm}^{-1}$,^{21c} and $\epsilon_{600}(\text{EDA complex}) = 530 \text{ M}^{-1} \text{ cm}^{-1}$,^{21c} a theoretical ratio of $(4300-640)/(2200-530) = 2.2$ was obtained for 1:1 cation/anion formation. The validity of the theoretical ratio in this case is very sensitive to the extinction coefficient of the relatively weak $\text{IN}^{\bullet+}$ absorbance. Full agreement between the experimental and theoretical ratios would be achieved if a value of $\epsilon_{600}(\text{IN}^{\bullet+}) = 2800 \text{ M}^{-1} \text{ cm}^{-1}$ were used.

For the quantitative analysis of the transient spectra of the photoexcited EDA complex of TCNE with styrene, the extinction coefficient of $\text{STY}^{\bullet+}$ was needed. All attempts to determine the extinction coefficient on the nanosecond time scale from electron-transfer quenching experiments with photoexcited chloranil^{7a,84} failed, probably because of the very rapid reaction of the styrene radical cation with neutral styrene.^{60,84} Thus, an alternative (picosecond) approach was chosen. The transient spectrum obtained 30 ps following the photoexcitation of the EDA complex of styrene with 1,2,4,5-tetracyanobenzene (TCNB) in dichloromethane showed the absorption bands of $\text{TCNB}^{\bullet-}$ and $\text{STY}^{\bullet+}$ at 470 and 600 nm, respectively. On the basis of $\epsilon_{470}(\text{TCNB}^{\bullet-})$ of $11\,600 \text{ M}^{-1} \text{ cm}^{-1}$,⁸⁵ the quantitative comparison of the two absorption bands yielded an extinction coefficient of $4800 \text{ M}^{-1} \text{ cm}^{-1}$ at $\lambda_{\text{mon}} = 600 \text{ nm}$ for the styrene cation radical. Using this value for $\epsilon_{600}(\text{STY}^{\bullet+})$, $\epsilon_{450}(\text{TCNE}^{\bullet-}) = 5700 \text{ M}^{-1} \text{ cm}^{-1}$,^{31a} $\epsilon_{450}(\text{EDA complex}) = 2170 \text{ M}^{-1} \text{ cm}^{-1}$,^{21c} and $\epsilon_{600}(\text{EDA complex}) = 150 \text{ M}^{-1} \text{ cm}^{-1}$,^{21c} a theoretical ratio of 0.76 was calculated for 1:1 formation of $\text{STY}^{\bullet+}$ and $\text{TCNE}^{\bullet-}$. This value was in excellent agreement with the experimental ratio of absorbances $A(450)/A(600) = 0.68$.

For a comparison of CT excitation and ET quenching data (see Figures 6 and 7), values for the ET driving force ΔG_0 were estimated for the CT ion pairs of TCNE with benzene and olefins. The driving force was calculated as the difference between the reduction potential of TCNE ($E_{\text{red}}^{\circ} = +0.24 \text{ V vs SCE}^{19}$) and the oxidation potentials (E_{ox}°) of the donors. The latter were either taken from the literature^{48,54} or extracted by interpolation from plots of E_{ox}° versus ionization potential by the method of Fleischmann and Pletcher.⁴⁹

Acknowledgment. We thank the National Science Foundation, the Robert A. Welch Foundation, and the Texas Advanced Research Program for financial support.

JA954242O

(84) Schepp, N. P. Johnston, L. J. *J. Am. Chem. Soc.* **1994**, *116*, 6895.

(85) The extinction coefficient of TCNB radical anion (in dichloromethane) was determined by the quantitative comparison of the absorption band of $\text{TCNB}^{\bullet-}$ with that of the biphenyl cation radical in the picosecond transient spectra observed upon excitation of the EDA complex of TCNB with biphenyl. For the extinction coefficient of biphenyl cation radical, see ref 7a. For the photoexcitation of the biphenyl/TCNB complex in acetonitrile see ref 37b.